

Characterizing the Dilemma of Performance and Index Size in Billion-Scale Vector Search and Breaking It with Second-Tier Memory

Rongxin Cheng^{1,2}, Yifan Peng¹, Xingda Wei^{*1,2}, Hongrui Xie¹, Rong Chen^{1,2}, Sijie Shen³, and Haibo Chen¹

¹Institute of Parallel and Distributed Systems, SEIEE, Shanghai Jiao Tong University

²Shanghai AI Laboratory

³Alibaba Group

Abstract

Vector searches on large-scale datasets are critical to modern online services like web search and RAG, which necessity storing the datasets and their index on the secondary storage like SSD. In this paper, we are the first to characterize the trade-off of performance and index size in existing SSD-based graph and cluster indexes: to improve throughput by $5.7 \times$ and $1.7 \times$, these indexes have to pay a $5.8 \times$ storage amplification and $7.7 \times$ with respect to the dataset size, respectively. The root cause is that the coarse-grained access of SSD mismatches the fine-grained random read required by vector indexes with small amplification.

This paper argues that second-tier memory, such as remote DRAM/NVM connected via RDMA or CXL, is a powerful storage for addressing the problem from a system's perspective, thanks to its fine-grained access granularity. However, putting existing indexes—primarily designed for SSD—directly on second-tier memory cannot fully utilize its power. Meanwhile, second-tier memory still behaves more like storage, so using it as DRAM is also inefficient. To this end, we build a graph and cluster index that centers around the performance features of second-tier memory. With careful execution engine and index layout designs, we show that vector indexes can achieve optimal performance with orders of magnitude smaller index amplification, on a variety of second-tier memory devices.

Based on our improved graph and vector indexes on second-tier memory, we further conduct a systematic study between them to facilitate developers choosing the right index for their workloads. Interestingly, the findings on the second-tier memory contradict the ones on SSDs.

1 Introduction

Multi-dimensional vectors with tens or hundreds of dimensions are powerful representations of multi-modal data including but not limited to text, vision, and videos [38, 40]. As a result, vector search—searching a database with numerous vectors to find the closest one given a query vector—is a key pillar in supporting real-world tasks like web search [32] and retrieval augmented generation (RAG) [30]. However, finding

the exact closest vector is often impractical, particularly for high-dimensional and large-scale vector datasets commonly found in real workloads [56, 8]. Therefore, systems typically use *approximate nearest neighbor search* (ANNS) to find an approximation of the k closest vectors in the dataset (i.e., find the $top-k$) [47, 60, 7, 6, 56].

A key system requirement for vector search is high performance. For example, vector search is the backend of Google search [9], a service that is latency sensitive [4, 11] and demands high processing rate: e.g., handles 8.5 billion queries each day [44]. To accelerate ANNS-based vector search, people have built two types of indexes: graph [47, 36, 15] and cluster [7, 14, 56]. Graph indexes use a configurable number of edges to link vectors that are close in distance, and conduct graph traversal to locate the $top-k$ vectors. Cluster indexes group closed vectors into clusters. They then perform a brute-force search on a configurable number of clusters to find the $top-k$ of a query vector.

For vector searches on large-scale datasets, it is common to store the graph and clusters on secondary storage like SSD [7, 56, 47]. As the SSD bandwidth is several orders of magnitude slower than DRAM, SSD-based vector search is *I/O bound*. For example, a commodity 64-core server can search 3,624–5,212 Mvectors/sec with SIMD¹ on common vector datasets with 100–384 dimensions. In comparison, an SSD with 5.3 GB/s bandwidth can only search 14–53 Mvectors/sec even considering its bandwidth is fully utilized (e.g., in cluster indexes). For indexes like graph, fully utilizing the SSD bandwidth is impossible due to the small random reads (e.g., 256 B).

The high performance and low index size dilemma for I/O-bounded vector searches. One intuitive way to improve I/O performance in existing vector indexes is to increase the index size, e.g., store extra information (edges and replicated vectors). For the graph, when the size of the graph is increased by adding more edges, the number of hops—each corresponding to a small random I/O—dramatically decreases. Meanwhile, as each hop reads more data (e.g., from 256 to 1024 B), the SSD bandwidth utilization also increases. For the cluster, by replicating vectors in adjacent clusters, the number of clusters required for the search [7, 56] also dramatically reduced, so

^{*}Xingda Wei is the corresponding author (wdxwfc@sjtu.edu.cn)

¹Single Instruction Multiple Data.

the overall search performance improves.

However, the index size required for optimal vector search is orders of magnitude higher than the traditional scalar indexes. For example, DiskANN [47] and SPFresh [56]—the state-of-the-art graph and cluster indexes—require indexes that are $4.9 \times$ and $6.7 \times$ larger than the indexed dataset (index amplification) for an optimal performance, respectively (§3). In comparison, scalar indexes like B⁺Tree or hash table only have an index amplification of $0.4\text{--}1.2 \times$ [59]². Unlike scalar indexes, the index size, the number of I/Os and the size of each I/O are determined by the machine learning algorithms that build the index and search it, which we argue can hardly improve to match the requirements of high-performance SSD accesses.

Another way to tackle this problem is from a system’s perspective without changing the algorithms. For example, we can deduplicate the replicated vectors in cluster indexes by replicating the address instead of vectors (§6.1), thereby reducing the cluster index with replication by 84%. However, naively changing the index layout could result in orders of magnitude more small random reads (100–384 B) to read replicated vectors, and the resulting performance is only 1.5% of the original replicated design on SSD.

Root cause: workloads mismatch SSD requirements. The workloads of graph or vector indexes with small amplification share the same characteristics: they are I/O intensive, require many random accesses over large datasets, and the sizes of reads are small, e.g., a few edges in the graph (e.g., 256 B) and a single replicated vector (e.g., 100–384 B) for cluster deduplication. The above workloads mismatch with the high bandwidth utilization requirements of traditional storage like SSD, i.e., using a few sufficient large reads (4 KB) to fully utilize the SSD bandwidth.

The second-tier memory for the rescue. We argue that second-tier memory—volatile or non-volatile (NVM) memory that is attached to the host with fast interconnects like RDMA and CXL [10] (§4), opens up opportunities to systematically address the problem. Specifically, these devices behave like storage but support finer access granularity (256 B vs. 4 KB), which matches the workload patterns of vector indexes. Moreover, they are robust to random reads with even smaller access granularity (e.g., 100 B). Specifically, adding 50% such I/O might not affect the memory bandwidth utilization, while in SSD the utilization drops by up to 43%. *Therefore, we can trade a few sequential accesses in vector search for dramatically reducing index size.*

Challenges and solutions for utilizing second-tier memory. In this paper, we built two indexes around the performance features of second-tier memory to show the effectiveness of vector indexes in second-tier memory. On various devices including RDMA, CXL, and NVM, our graph index can

²The database community still believes that such an amplification is huge [59].

reach the optimal performance with 4–44% less index storage, and our cluster index can achieve so with 40% index size amplification.

Achieving so is non-trivial. First, existing billion-scale vector indexes are designed for SSDs, so they cannot fully utilize the fine-grained access nature of second-tier memory. Second, treating the second-tier memory as DRAM also results in poor performance because they still behave like storage devices, e.g., with an order of magnitude higher latency and should minimize the number of small reads. For example, placing the graph index on second-tier memory would shift the performance bottleneck from I/O to computation, but the relatively long access latency of second-tier memory hinders the CPU from fully utilizing the SIMD for vector search (§5). Therefore, we retrofit the execution pipeline of the graph index to hide the execution delay caused by reading the second-tier memory. Meanwhile, naively deduplicating the cluster index would result in numerous small random I/Os on the second-tier memory. This prevents us from fully utilizing the I/O bandwidth (§6). To this end, we designed a grouping mechanism to minimize the small random I/Os on second-tier memory.

An end-to-end study on comparing graph and vector indexes (§7). To conclude our study of utilizing second-tier memory for vector indexes, we conducted a systematic study comparing the graph and cluster indexes on second-tier memory. We draw several interesting findings that contradict common findings on SSD. First, it is widely known that graph is slower than the cluster because it is unfriendly to the SSD’s I/O, which causes its poor performance [7, 56]. However, graph can have much better performance than the cluster, not only because its I/O is more efficient on second-tier memory, but also it reads far fewer vectors than the cluster. Second, the cluster index is notoriously for huge index size ($6.3\text{--}7.7 \times$ of original dataset) caused by replication [49]. On the second-tier memory, with our improved design, the index size can be kept consistently small ($1.1\text{--}1.4 \times$).

Contributions. In summary, our contributions are:

- We are the first to characterize the high performance and low index size amplification dilemma in SSD-based indexes for large-scale vector datasets.
- We provide the first guideline on how to utilize second-tier memory for breaking the aforementioned problem.
- We built the first graph and cluster indexes on second-tier memory that achieve orders of magnitude higher performance as well as orders of magnitude smaller index size.
- We present the first end-to-end study comparing the graph and vector indexes on second-tier memory.

2 Vector Search and Second-tier Memory

2.1 ANNS-based vector search and its indexes

ANNS-based vector search. Given a query vector and a vector dataset, vector search finds the most similar vector in

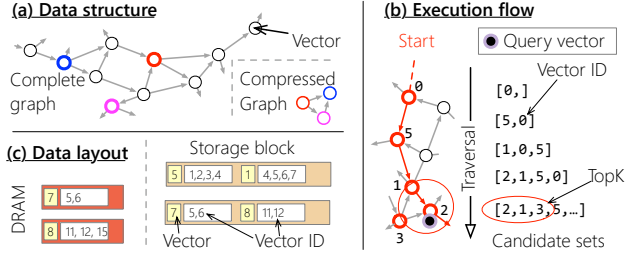


Figure 1: An illustration of (a) the basic data structures of graph-based vector index, (b) the execution flow of vector search with it and (c) how the data structures are stored.

the dataset. Formally, given a vector dataset $[x_1, x_2, \dots, x_n]$ and a query vector x , where $x \in \mathbb{R}^d$, the search will find $x_i = \operatorname{argmin}_{x_i} \operatorname{dist}(x, x_i)$, where dist is the distance metric, e.g., Euclidean distance. Due to the curse of dimensionality [8], it is impractical to find the exact x_i especially for high-dimensional vectors commonly found in real-world applications [7, 56, 60]. Therefore, systems conduct *approximate nearest neighbor search (ANNS)* for the vector search, which finds K approximate nearest candidates for the x_i (*top- k*). To accelerate ANNS, people have built two types of indexes³:

Graph-based index [47, 36, 15]. It stores vectors in a directed graph (Figure 1 (a)), where the nodes are vectors and the edges connect vectors that are close in distance. For example, if $a \rightarrow b$, it means that vector b is the *top- k* vector of a . Figure 1 (b) presents the execution flow of the search. The search begins at a start node in the graph and identifies the nearest neighbors through best-first graph traversals. Specifically, each hop in the traverse will read a vector and its edges from the storage. The starting node of the traverse can be fixed [15], chosen randomly [33, 1] or selected by traversing a (relative) small or compressed graph that is distilled from the original graph [36, 47, 42] (see (a)). During the traversal, the search maintains a candidate set containing the closest vectors traversed so far (sorted by their distances). After the traversal is completed, the search returns the *top- k* results from the candidate set as the final *top- k* results of the search. The traversal stops as long as the candidate set size exceeds a pre-defined threshold (a hyperparameter).

The full graph is typically stored as adjacent lists in the secondary storage [47, 42], as shown in Figure 1 (c). Note that the nodes and edges are stored together since each traversal requires both data. On the other hand, the compressed graph, which aids in traversal, is stored in the DRAM [47].

The benefit of a graph index lies in its ability to capture the relationships between vectors in a fine-grained way. As a result, the search process has *low read amplification*, meaning it reads only a few extra vectors beyond the required *top- k* . The downside is that graph traversal is not friendly to storage

³To the best of our knowledge, no other types of billion-scale vector indices exist.

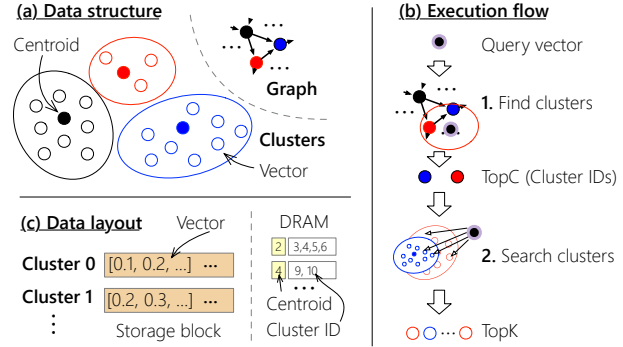


Figure 2: An illustration of (a) the basic data structures of cluster-based vector index, (b) the execution flow of vector search with it and (c) how the data structures are stored.

due to its pointer chasing access pattern, resulting in long latency and low bandwidth utilization [7, 56]. Moreover, the graph index is not friendly to vector insertions, as building the graph necessitates reconstructing the graph [56].

Cluster-based index [7, 14, 56]. The cluster index has been optimized for storage access. As shown in Figure 2, The vectors are partitioned into clusters where each cluster can be stored efficiently in a storage block (e.g., an SSD block), as shown in Figure 2 (c). The search then only needs to read the closest clusters to get the *top- k* . To facilitate finding the closest clusters, cluster indexes typically use a graph index to record the cluster relationships, where the graph node is the centroids of the clusters [7, 56, 29]. Since the graph is typically much smaller than the cluster (only contains centroids), it is stored in memory for efficient search. Figure 2 (b) presents the concrete execution flow. The search first traverses the graph to find the *top-c* clusters. Afterward, it reads all the cluster data and searches the *top-k* among them.

The benefits of cluster-based indexes include: (1) they are efficient for secondary storage as they allow large bulk reads of clusters, and (2) they are friendly to insertion workloads, as vectors can be inserted into the closest clusters without the need for rebuilding the whole index like graph [56]. However, cluster-based indexes have *high read amplification* due to redundant vectors read in each cluster. Meanwhile, they also have *high space amplification* due to replications required for high accuracy (see §2.2 for more details).

2.2 Building vector indexes

The space consumed by vector indexes is closely tied to how the indexes are constructed. Both types of indexes are built using traditional unsupervised machine learning methods.

Graph-based index. To build a graph index on a dataset of vectors, the builder first uses k-Nearest Neighbor (*kNN*) to find the closest neighbors for each vector. The k is a static user-configured parameter for index construction. Note that this k is unrelated to the *top- k* required by the query. It then

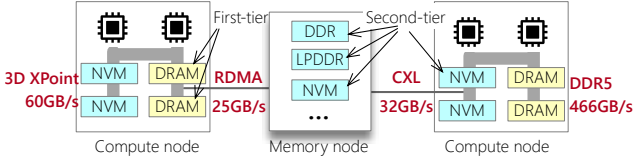


Figure 3: First-tier memory vs. second-tier memory.

Table 1: Performance features of different memory technologies.

| | SSD | DRAM | RDMA | CXL | NVM |
|-----------|------------|-------------|-------------|-------------|-------------|
| Bandwidth | 5.3 GB/s | 35 GB/s | 25 GB/s | 32 GB/s | 60 GB/s |
| Latency | 75 μ s | 0.1 μ s | 2.8 μ s | 0.3 μ s | 0.4 μ s |

connects each vector with its k closest neighbors to form the graph. Graph indexes typically choose a small k (e.g., 32 [47]) as it could significantly amplify the space of the index (see §3). Based on the graph formed by kNN , existing indexes also prune the edges using methods like sparse neighborhood graph (SNG) [3] for improved traversal quality.

Cluster-based index. First, the builder partitions the vectors into clusters using *kMeans*. The number of clusters is selected to be orders of magnitude smaller than the number of vectors. One issue with *kMeans* is that it can cause unbalanced partitioning, i.e., one cluster may contain significantly more vectors than others. Unbalanced clusters can lead to high variance in search time, so state-of-the-art indexes [7, 56] will further balance the cluster size using a multi-constraint balanced clustering algorithm [34]. Another issue with *kMeans* is the boundary issue. Specifically, boundary vectors of a cluster can be assigned to multiple neighboring clusters. However, *kMeans* assigns them to only one cluster. Ignoring this issue leads to searching through more clusters for accuracy, which further results in significant performance degradation. Therefore, existing indexes replicate boundary vectors to a set of close clusters, where the number of replications is statically configured before the index build.

2.3 Second-tier memory

Figure 3 presents the second-tier memory architecture that we target in this paper. Unlike traditional fast DRAM that is directly connected to the CPU via the memory bus, second-tier memory is a relatively slower, but cheaper memory device that can be indirectly connected to the CPU through a high-bandwidth interconnect like RDMA [63, 16] or CXL [10, 37]. The memory can be either old-generation DRAM (DDR3), which is sufficient to saturate the interconnect bandwidth, or persistent memory like NVM [22, 53]⁴. They have less cost per GB compared to locally attached DRAM because: (1) older-generation memory is cheaper and (2) indirection allows improved memory utilization by pooling unused memory [31, 61, 19]. However, they are still significantly slower than DRAM and behave more like storage (detailed in §4): They require a sufficient large request payload (e.g., 256 B)

⁴NVM can also be directly attached to the CPU like DRAM.

Table 2: Billion-scale datasets used in the experiments.

| Dataset | Dataset | Dimensions | Total space | Queryset |
|------------|-----------|---------------------|-------------|----------|
| SPACEV (S) | 1 Billion | 100 \times int8 | 94 GB | 29 K |
| BIGANN (B) | 1 Billion | 128 \times uint8 | 120 GB | 10 K |
| DEEP (D) | 1 Billion | 96 \times float32 | 358 GB | 10 K |

to saturate the interconnect bandwidth (see Figure 6).

To show that our results generalize to a variety of second-tier memory, we considered all three known implementations in production (see Table 1): RDMA-attached DRAM (RDMA), CXL-attached DRAM (CXL), and NVM.

3 The Dilemma of High Performance and Small Index Size in Vector Indexes

Setup, datasets and baseline indexes. We conducted experiments on a machine equipped with an Intel D7-P5520 SSD (7.7 TB, 5.3 GB/s),

and an Intel Xeon Gold 6430 CPU (20 cores, 3.4 GHz). We use three popular billion-scale workloads used by existing works [47, 7, 56]—the largest publicly available datasets for vector search (see Table 2).

We choose two vector search systems as our baselines:

- **Graph (DiskANN [47]).** DiskANN is the state-of-the-art graph index. It follows the graph index design described in §2.1, and further leverages product quantization (PQ) to compress the graph in memory to accelerate graph search.
- **Cluster (SPFresh [56]).** SPFresh is state-of-the-art cluster index that utilizes: (1) an in-memory graph index on centroids to accelerate finding search clusters for the query vector, and (2) a balanced partitioning algorithm to ensure low variances in cluster sizes. Additionally, SPFresh supports in-place updates.

Both indexes are optimized with SSD access, e.g., they use SPDK [45] to achieve the best I/O performance on SSDs, and leverage SIMD for execution.

Search accuracy and runtime index hyper parameters. The accuracy of the vector index is defined in terms of *recall*, i.e., the ratio of result vectors returned by the index in the ground-truth *top-k*. Given the same accuracy, the performance of vector search is strongly influenced by the configuration of its runtime hyperparameters, i.e., the number of clusters to search and the maximum size of the candidate set (that determines the graph traversal hops, see Figure 1 (b)).

Like prior work [7, 56, 47], we choose the parameters that achieve the best performance at a given accuracy level, and use an overall accuracy of at least 90% across all experiments. Note that for a given dataset and index, its hyperparameters are configured only once and remain unchanged during its query time.

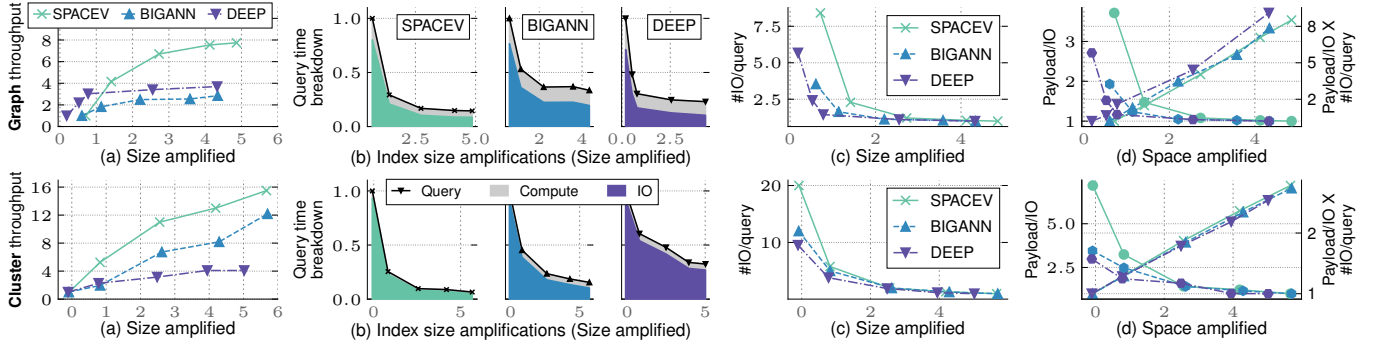


Figure 4: (a) Performance—index size trade-off in existing graph-based (upper) and cluster-based (bottom) vector indexes. The amplification is normalized to the total dataset size without indexing. (b) I/O dominates index performance across various datasets. (c) The performance increases when the index size becomes larger is due to the reduced number of I/O sent per-query and (d) the request payload per I/O and its trend compared to the reduced number of I/O per query. Note that all the performance data is normalized.

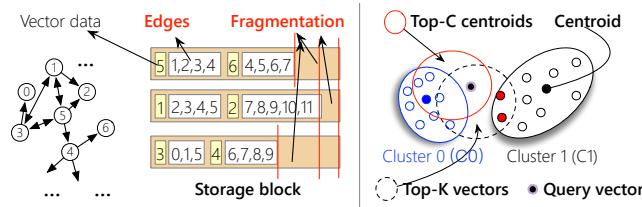


Figure 5: An illustration of (a) the index size amplification problem in graph indexing and (b) why a cluster index requires replication.

3.1 Case study: graph index

Sources contribute to the index size. Similar to a traditional graph, the additional space occupied by the graph vector index comes from two sources: the space used to store graph edges, and the internal fragmentation that prevents cross-storage block graph traversal (see Figure 5 (a)). The space for edges is non-trivial and dominates the amplification: For every vector in the dataset, the graph stores edges as adjacency list next to it (the graph is sparse). For instance, DiskANN by default assigns 32 edges to each vector. Given that each edge is a 4 B vector ID, the size of the list can exceed the original data (e.g., 128 vs. 100 in SPACEV). Specifically, DiskANN by default introduces an 0.5–1.4 × space amplification in existing datasets. Note that this relatively small amplification trades graph traversal performance, which we will elaborate on later.

Unlike other graph systems like graph databases and analytics, where the number of edges cannot be controlled by the system, the graph vector index can configure different numbers of edges per vector, providing control over the space used by the graph. Specifically, we can adjust the k in the KNN algorithm used to build the graph (see §2.2) to control the number of edges per vector.

Characterizing the problem. Ideally, we should minimize the space amplification caused by edges. Unfortunately, the fewer the edges, the longer the path a query vector must traverse to find its approximate *top-k*. Since an SSD access

is orders of magnitude slower than computing the distance between two vectors (e.g., 70 μ s vs. 1 ns on our platform), such extra hops significantly slow down the search in graph index, see Figure 4 (b). Therefore, the graph index faces a fundamental dilemma of high performance and low index size. More specifically, since I/O dominates the graph search, the performance of the graph index can be characterized as:

$$\text{Throughput}_{\text{search}} = \text{Band.} / (\# \text{Hops} \times \text{Size}_{\text{node+edge}}) \quad (1)$$

For our evaluated dataset, the payload read ($\text{Size}_{\text{node+edge}}$) per graph traversal (Hop) cannot exceed the SSD access granularity (4 KB) even if we increase the number of edges, because otherwise would result in a large index size that is 39 × larger than the original dataset, e.g., using 100 B for the node and 3,996 B to store the edges. As a result, the achieved bandwidth (Band.) divided by ($\text{Size}_{\text{node+edge}}$) can be simplified as the IOPS of the storage device—the maximum requests per second that the SDD can handle. So we can simplify the performance model 1 as:

$$\text{Throughput}_{\text{search}} = \text{IOPS} / \# \text{Hops} \quad (2)$$

The model clearly shows that when we increase the number of edges of graph indexes, the number of hops required for traversal decreases, so the throughput increases.

The upper half of Figure 4 (a) shows the empirical vector search performance respective to the index size (measured with size amplification) for all datasets. Take SPACEV dataset as an example, other datasets share a similar result. When the index size increases from 1.7–5.9 ×, the throughput increases from 1.9–15.2 Kreqs/sec, and the peak throughput is 1.9 × faster than the DiskANN’s default setup (#Edges/vector=32). The performance improvement is due to the reduced number of hops required for traversal (see Figure 4 (b)): the number of I/O per query decreased significantly from 350 to 37. Even though each I/O reads more data from the SSD, which increases from 164–580 B for the index when sizes grow from 1.7–5.9 × of the size of SPACEV, the performance still dramatically improves. This is because the IOPS remains

steady (see Figure 4 (d)), since such payloads are still far from saturating the SSD bandwidth.

3.2 Case study: cluster index

Sources contribute to the index size. Unlike a graph index, cluster index should ideally have negligible index size. This is because (1) the index data used for recording clusters are orders of magnitude smaller than the total datasets (one cluster for every tens or hundreds of vectors) and (2) clusters stored on the SSD are more resilient to cross block accesses (since each cluster may cross block due to its large size) so no padding is necessary. Unfortunately, state-of-the-art cluster indexes [7, 56] extensively replicate a single vector across multiple clusters to address the loss of accuracy caused by the *boundary issue* (see Figure 5 (b)). In this example, the *top-k* of the query vector spans the boundaries of cluster 0 and 1. If the *top-c* centroids only contain cluster 0, then the red vectors from cluster 1 will be missed from the final *top-k*, causing reduced accuracy.

Replicating the boundary vectors to both clusters addresses the issue, at the cost of additional storage used for the index. In general, the higher the replication factor, the better the accuracy. Unfortunately, the number of replications that can be achieved is limited because the replication is applied globally to all vectors in the dataset. For example, SPFresh [56] set a maximum replication factor of 8, which in the worst case would amplify the space by $8 \times^5$.

Characterizing the problem. To avoid excessive replication, another solution is to increase the number of clusters searched for each query. For instance, if we search both cluster 0 and 1 as shown in Figure 5 (b), we can achieve the same accuracy without replication. Unfortunately, additional cluster searches obviously degrade the vectors searched due to the extra vectors read.

Similar to the graph index, I/O dominates the throughput of cluster vector search (the bottom of Figure 4 (b)), which can be characterized as:

$$\text{Throughput}_{\text{search}} = \text{Band.} / (\# \text{Clusters} \times \text{Size}_{\text{cluster}}) \quad (3)$$

Band. is the bandwidth of the device, and #Clusters is the configured number of searched clusters per query.

Unlike the graph index, the cluster size can exceed the SSD payload threshold (4 KB), so we cannot simply use the IOPS to characterize the search throughput. When considering the request payloads, the relationship between the index size and the throughput is more complex to analyze. As shown in Equation 3, increasing the index size would increase the average cluster size as well as reduce the number of clusters searched. Nevertheless, empirically we found the number of

⁵Existing indexes prune replicated vectors to reduce index size [7, 56]. However, pruning does not fundamentally change the amplification factor caused by replication, e.g., only reduces the amplification from 7 to 5.7–6.3 in the datasets.

clusters required to search (#Clusters) decreases more than the increase in the average cluster size, so increasing the index size can still improve the throughput.

The bottom of Figure 4 (a) shows the performance–index size graph of cluster index. For BIGANN and SPACEV datasets, the throughput increase $12 \times$ and $16 \times$ when we increase the index size by $7.3 \times$ and $7.2 \times$, respectively. For DEEP, the throughput increase $4 \times$ when increasing the index size by $6.7 \times$. All datasets achieve their peak throughput when configured with a replication factor of 8, the maximum supported by SPFresh. The performance improvement is due to fewer clusters being searched (Figure 4 (c)). For instance, in BIGANN, it only requires searching 20 clusters to achieve 90% accuracy with a replication factor of 8. In comparison, with a replication factor 1, it has to search 240 clusters. Such a reduction in the number of clusters searched offsets the reduced IOPS caused by the increased payload per cluster (see the bottom of Figure 4 (d)).

3.3 Root cause: workloads mismatch SSD requirements

We attribute the dilemma to a mismatch between the I/O requirements for high-performance SSD access and I/O workloads issued by vector indexes with small index amplification.

Graph index requires fine-grained storage reads for practical index sizes. For a practical graph index with minimal index size, we must construct it with a small number of edges per node. From an algorithmic perspective, this means that graph traversal must use random I/Os with small payloads to read these edges. However, this fundamentally conflicts with the requirement of using a sufficiently large I/O payload (4 KB) to efficiently utilize traditional storage devices like SSD.

Cluster index requires irregular I/O for deduplication. For cluster indexes, we can deduplicate vectors through indirection. Specifically, instead of storing replicated vector data in other clusters, we store an address pointing to the original cluster. As the vector address (8 B) is significantly smaller than the data (128–384 B), this approach minimizes index size. However, it implies that each replicated vector requires a separate small random read (100–384 B) to fetch the original vector. Such an I/O pattern is irregular to the SSD: 50% can cause 43% performance drop.

4 The Power of Second-tier Memory in Vector Search

We now explain our rationale for using second-tier memory for vector indexes, whose access features perfectly match the I/O patterns of vector indexes.

1. **Fine-grained block sizes⁶:** Compared to traditional storage like SSD, second-tier memory has a more fine-grained

⁶We use block size to denote the smallest access granularity of second-tier memory, without losing generality.

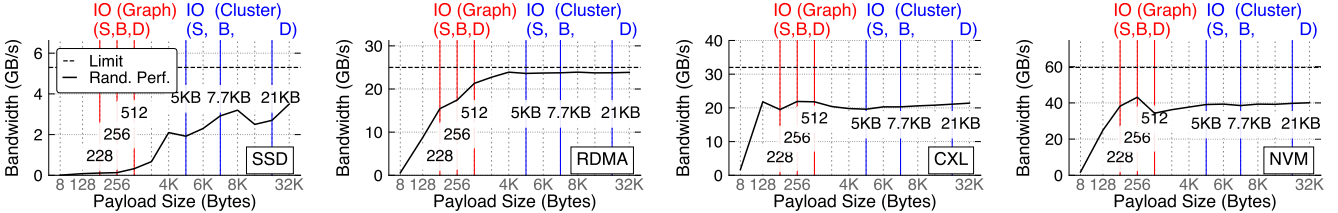


Figure 6: A comparison of peak random read performance using various read payloads for SSD and different second-tier memory hardware. Note that the x-axis is non-linear. For reference, we also mark the typical read payload of the graph (red lines) and cluster (blue lines) index for SPACEV (**S**), BIGANN (**B**), and DEEP (**D**) datasets.

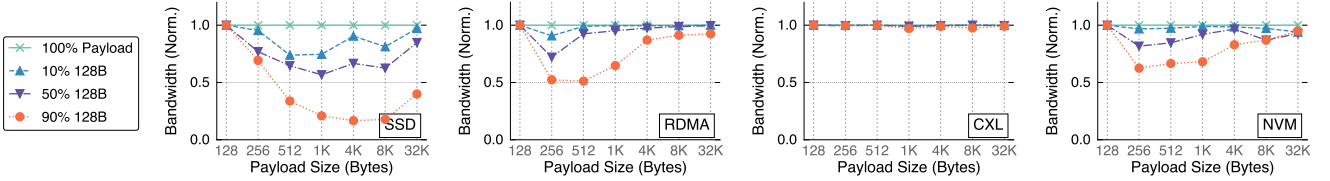


Figure 7: An analysis of the slowdown introduced by random 128 B reads for various devices.

Table 3: Measurement machines with second-tier memory.

| Platform | Host CPU configuration | Second-tier Memory |
|----------|--|--|
| RDMA | Intel(R) Xeon(R) Gold 6430 (32 cores, 3.4 GHz) | BlueField-3 200 Gbps (up to 25 GB/s) |
| CXL | Intel(R) Xeon(R) Platinum 8468V (48 cores, 3.8GHz) | MXC CXL Memory eXpander (CXL 2.0), PCIe 5.0 x8 (up to 32 GB/s) |
| NVM | Intel(R) Xeon(R) Gold 6330 CPU (28 cores, 2.0GHz) | 8 × Optane 200 Series (up to 60 GB/s) |

block size (from 64–256 B). Such a pattern matches the requirements of vector indexes, e.g., graph reads 228–512 B for each traversal, which means that vector index can utilize the device bandwidth more efficiently.

2. **Robust to irregular I/Os:** The measured performance is robust against large payloads unaligned with the device’s access granularity, and random reads with not-so-small payloads (e.g., a single vector that is 128 B), which is common for vector indexes with small sizes. Vector indexes don’t issue other patterns of irregular payloads (e.g., 8 B random reads).

The aforementioned advantages give us opportunities to break the space–performance dilemma in existing index designs systematically. First, the fine-grained I/O access granularity of second-tier memory matches the graph index requirements—small random reads for low space amplification. Second, we can utilize the robustness of irregular IO to replace (some) sequential accesses with random accesses. Therefore, we can effectively deduplicate the cluster index storage to achieve minimal index size.

Characterized second-tier memory and experiment setup.

To show that our results generalize to various second-tier memory hardware, we use three machines, each with a dif-

ferent memory technique⁷, (Table 3) through all experiments. The machines are named after the memory technique.

We use two microbenchmarks: the first measures the random access performance of various devices, while the second evaluates the performance when a portion of the workload is replaced with irregular payloads, i.e., small 128 B random access. We chose 128 B because it represents the common payload (a single vector) used in both vector indexes (see Table 2). For each device, we have carefully tuned the performance to avoid inference from underutilized hardware. For SSD, we use SPDK to implement both benchmarks. For RDMA, we built index on a state-of-the-art RDMA framework [52] with all known RDMA-aware optimizations [12, 27, 52]. For CXL and NVM, we utilize devdax for direct device access and apply all guidelines summarized in existing studies [57, 54].

Fine-grained access granularity that matches vector index searches. Figure 6 shows the bandwidth achieved on different devices using various payloads. First, SSD requires a sufficiently large payload (multiple of 4 KB) to approach its bandwidth limit, which is not aligned with the typical vector index payloads. For instance, the graph index, when configured with 32 edges per node for small amplification by default, issues reads in 228–512 B payloads for various datasets. In contrast, all second-tier memory devices can saturate the bandwidth with relatively small payloads: RDMA, CXL, and NVM can achieve close to bandwidth limit with payloads of 4 KB, 128 B, and 256 B, respectively.

The differences lie in the underlying hardware design. Compared to RDMA, CXL, and NVM, which have block size of 64 B, 64 B and 256 B respectively, SSD has a larger block size of 512 B. Additionally, issuing random access with SSD block size is insufficient to saturate the bandwidth, as SSDs have multiple flash dies that process 512 reads sequentially.

⁷One machine cannot be equipped with all three techniques due to the specialized motherboard required for CXL and NVM.

Therefore, a large read payload (i.e., 4 KB) enables the SSD to distribute reads more evenly across the dies, thereby improving performance with reduced die collisions [26].

Robust to irregular IO. SSDs are not robust to irregular payloads including: (1) large payloads not aligned with the device’s block size (e.g., graph traversal in graph index), and (2) payloads smaller than the block size (e.g., graph traversal and reading a vector). As shown in Figure 6, SSD performance drops when using 5 KB, 7.7 KB, and 21 KB, which are extensively used by the graph index under different workloads. Figure 7 further shows that when the ratio of 128 B random read increases from 10–90% in the workloads, the SSD experiences 4.6–83.3% slowdowns.

In comparison, second-tier memory has small or no slowdown under similar scenarios. For (1), they experience no slowdown (see Figure 6). For (2), as shown in Figure 7, RDMA and NVM experience a maximum slowdown of 48.8% and 37.5% under an extreme setup where the workloads are 50% and 90% workloads are 128 B random reads. Second-tier memory is more robust due to its fine-grained block size, i.e., the bandwidth wasted is minimal. For example, for 228 B reads required by the graph, the worst waste is at 11% on NVM, while it is 55% on SSD, even without considering die collisions. Finally, RDMA is less robust when handling small random access due to the increased network protocol overhead for each request [18]. This suggests that reducing irregular access to second-tier memory remains necessary.

5 Improved Graph Index Design

Putting graph indexes on the second-tier memory can dramatically improve the index performance thanks to its features. However, existing system designs for graph indexes do not match or fully utilize the increased I/O capability of second-tier memory, causing performance under-utilization as well as storage waste. To this end, we propose two designs for graph index on the second-tier memory:

1. **Software pipeline.** With improved I/O performance, the computing capability becomes the performance bottleneck. Existing synchronous search design fails to fully utilize computational power, so we still need a large index to amortize the second-tier memory access latency. We propose a software pipeline mechanism to asynchronously process I/O with computation, thereby maximizing the use of computational power.
2. **Compressed graph layout.** The existing graph index suffers from internal fragmentation to avoid cross-SSD block access. The overhead space is trivial for graphs with large amplification, but it is significant when using a small-sized index on second-tier memory. Observing that second-tier memory is robust against irregular I/Os with unaligned access payloads (§4), we use a compact storage layout when storing graph indexes on it.

Software pipeline. The latency of second-tier memory is on the order of 300–3000 ns, which is much higher than that of first-tier DRAM (100 ns). This causes significant idle time if the CPU processes the I/O synchronously, as in the existing design: it busy waits for the I/O to complete before doing the computation—compare the distances of candidates with the vector node read back.

To this end, we interleave memory access and vector distance computation from multiple queries to hide the second-tier memory access latency⁸. Specifically, we schedule multiple queries execution in a per-hop way for inter-query parallelism: after issuing a second-tier memory request, we will schedule the execution of next unfinished query, thereby processing different queries in a pipelined way in software. Note that our software pipeline is different from batching because we won’t wait for a batching window before processing a query: the query is processed as soon as possible. For RDMA, we leverage coroutines [28] to implement such a feature. For CXL and NVM, since their memory accesses are implicitly issued via CPU load instructions, we will reorganize the instruction orders in the search to conduct a batch of loads before executing computation, as well as use `mm_prefetch` to realize the feature.

Figure 8 shows the performance improvement of the software pipeline. For RDMA, the software pipeline improves the performance by 1.2–1.6 ×. On CXL and NVM, the pipeline can also improve the performance by up to 1.2 ×. The improvements of the pipeline are more obvious in RDMA since it has the highest latency.

Compressed layout. One significant design choice in DiskANN is to use padding for storage: without it, DiskANN suffers a 48–58% performance loss on SSD. Such a padded design might waste 4–44% index spaces, as shown in Figure 8 (d)–(f). It is unnecessary on the second-tier memory thanks to its robustness to irregular I/O that cross-block size. Therefore, we simply choose a Compressed Sparse Row (CSR) layout [43] for storing the graph index on the second-tier memory. As also shown in Figure 8, CSR reduces space without compromising performance.

Overall performance. Figure 9 shows the end-to-end performance of the graph index on RDMA, CXL, and NVM with all the above optimizations enabled⁹. We calculate the computation bound by performing all calculations when storing the graph in DRAM and bandwidth bound by with the peak bandwidth measured in Figure 6. On second-tier memory, we can see that fine-grained random reads won’t cause significant bandwidth waste, so graph index can reach the CPU’s computation bound with a small index size amplification (1.7–4.1 ×)

⁸Interleaving does not help SSDs since the I/O is the bottleneck.

⁹Due to limited memory on our platform, we only report performance of 100M datasets for CXL and DEEP100M for NVM.

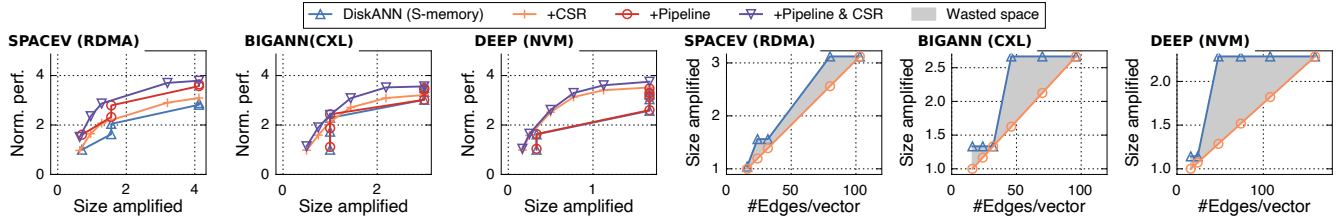


Figure 8: Effects of software pipeline (a)–(c) and CSR (d)–(f) on graph index. Due to space limitation, we only list a subset of the overall results. The trends for the others are similar.

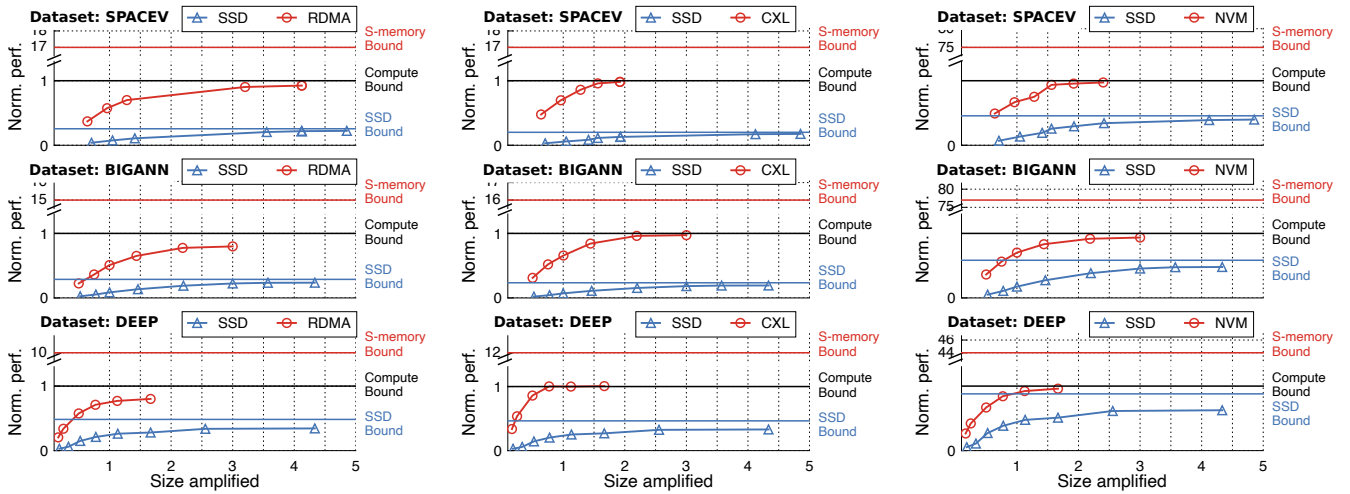


Figure 9: End-to-end graph index performance. S-memory states for second-tier memory used.

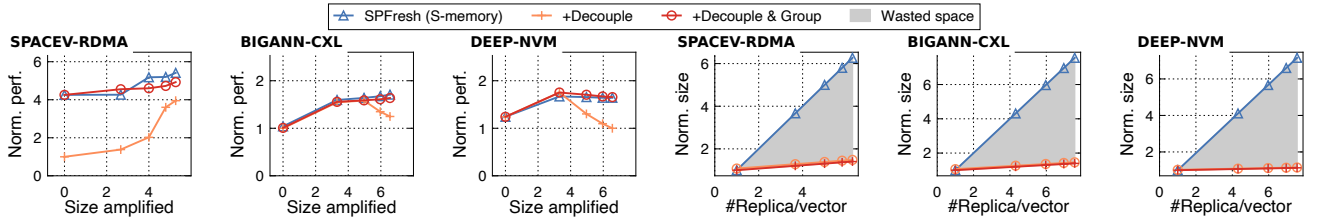


Figure 10: Effects of cluster-aware grouping (a)–(c) and decoupled layout (d)–(f) on graph index. Due to space limitation, we only list a subset of the overall results. The trends for the others are similar.

compared with SSD (4.3–4.9 \times to achieve optimal performance). Moreover, its performance is 2.3–4.1 \times higher than SSD.

6 Improved Cluster Index Design

To break the trade-off between index space and performance, we propose two system designs for placing the cluster index efficiently on the second-tier memory:

- Decoupled index layout (§6.1).** We store the vectors and clusters separately on the second-tier memory. Thus, the index build algorithm can replicate vectors (with high factors) in clusters with negligible index size amplification.
- Cluster-aware grouping (§6.2).** Decoupled layout inevitably introduces irregular I/Os on the second-tier mem-

ory, which can degrade performance if there are too many. Therefore, we propose a cluster-aware grouping algorithm to reorganize the vector layout post-index build to reduce such I/Os.

6.1 Basic design: Decoupled layout

To resolve the dilemma of high-performance and low cluster index size, we deduplicate the cluster index with a decoupled layout. As shown in Figure 11, unlike the existing cluster index that directly stores the (replicated) vectors in each cluster (a), we store vectors separately with the cluster data, and only store the addresses of vectors in each cluster (b). As a result, for replicated vectors, we only replicate the address. Since the address size is orders of magnitude smaller than a vector (8 B vs. 100–384 B vectors), replicating addresses has trivial

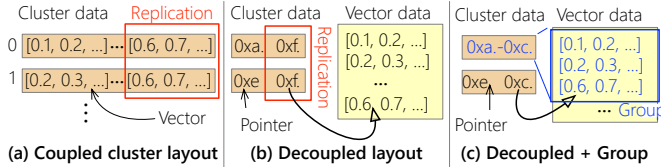


Figure 11: An overview of how we improve the layout of the vector index on the second-tier memory, from the traditional coupled design (a), to a decoupled design (b), and to a design with grouping (c).

Table 4: Variables used in the vector group algorithms. The optimization variable is determined by the algorithm, and constant variables come from the index build.

Constant variables:

$A_{i,j}$ If $A_{i,j}$ is 1, it means that the i_{th} vector is partitioned or replicated to the j_{th} cluster's.
 h_i The access frequency of the i_{th} 's cluster.

Optimization variable:

$P_{i,j}$ If $P_{i,j}$ is 1, it means that the i_{th} vector belongs to the j_{th} cluster's group.

storage overhead to the index (see (d)–(f) in Figure 10).

The execution flow of the index search is the same as with the decoupled layout. The only difference is that when reading a cluster, we will first read the vector addresses belonging to the cluster, and then issue separate reads to fetch the vectors. Those reads are small random reads with 100–384 B payloads, which is not efficient for traditional storage like SSD but is much more efficient on the second-tier memory.

Problem: too many irregular I/Os. Though the decoupled layout can reduce the index size, it also decouples the original 0.1–2.2 MB I/O in to $60\text{--}68 \times$ small random I/Os (100–384 B). More specifically, 98% of the I/Os in the workloads are small random I/Os, which are also inefficient on the second-tier memory (see Figure 7). As a result, we observe a 27–39% performance drop on all the workloads when increasing the replication factor (see Figure 10 (a)–(c)). Note that improving the replication factor is still important for an optimal index size.

6.2 Cluster-aware grouping

To reduce the number of small I/Os in the workloads, we propose vector grouping atop of the decoupled design to minimize the number of small random I/Os. By grouping the vectors belonging to the same cluster together and storing them in adjacent storage, we can use one large I/O to read all vectors in the group (see Figure 11 (c)). The group is done post the index build.

Since we don't replicate vectors, there must exist clusters that we cannot use one I/O to read all its vectors, e.g., when searching the cluster 1, we still need to use a separate small I/O to read the vector data belonging to address 0xc. Therefore, the performance of grouping heavily depends on how the

vectors are grouped. The vector group problem aims to determine which vectors should be grouped together to minimize small IOs in a given workload. It is equivalent to the problem of assigning vectors to specific cluster groups. Assume we have a vector database with a set of vectors V and a set of clusters C . We use $P_{i,j}$ to denote whether i_{th} vector has been assigned to a group.

We employ an integer linear program (ILP) to find the best group of $P_{i,j}$. The objective is to minimize the IO requests sent to the MN. Since the number of IOs depends on the access frequency of each cluster, we use h_j to denote the access frequencies of clusters. The frequencies can be obtained by monitoring the workload in the background, and we can dynamically change the layout according to frequency changes. Since dynamic adjustment is not the focus of our work, we will omit it in this paper.

Putting it all together, we formulate the problem as follows:

$$\begin{aligned} \text{minimize} \quad & \sum_j^{|C|} h_j \cdot \left(1 + \sum_i^{|V|} P_{ij}\right) \\ \text{subject to} \quad & \text{Cluster constraints} \\ & \text{Group constraints} \end{aligned} \quad (4)$$

Cluster constraints. According to the cluster index design, a vector must be assigned to one cluster, while being replicated to multiple adjacent clusters of the assigned cluster. We formulate the constraints as follows:

$$\begin{cases} 0 \leq A_{i,j} \leq 1, & i \in [0, |V|], j \in [0, |C|] \\ \sum_j^{|C|} A_{i,j} \geq 1, & i \in [0, |V|] \end{cases}$$

Group constraints. The group algorithm must assign a vector to exactly one cluster's group:

$$\begin{cases} 0 \leq P_{i,j} \leq 1, & i \in [0, |V|], j \in [0, |C|] \\ \sum_j^{|C|} P_{i,j} = 1, & i \in [0, |V|] \end{cases}$$

Solve the algorithm at billion-scale. One simple way to solve the problem is to use an off-the-shelf solve [24]. However, for billion-scale vectors, it takes non-trivial time to solve the problem (at least polynomial complexity). Observing the simple structure of the problem, we can use a simple greedy algorithm to find the optimal solution. Specifically, for a vector that has been replicated to multiple clusters, assigning it to the cluster with the highest access frequency is the optimal choice. This is because, informally, assigning it to a less frequently accessed cluster will increase the number of I/Os. Due to space limitation, we omit the detailed proof. As a result, we can quickly solve the problem even for billion-scale vectors in <90 minutes.

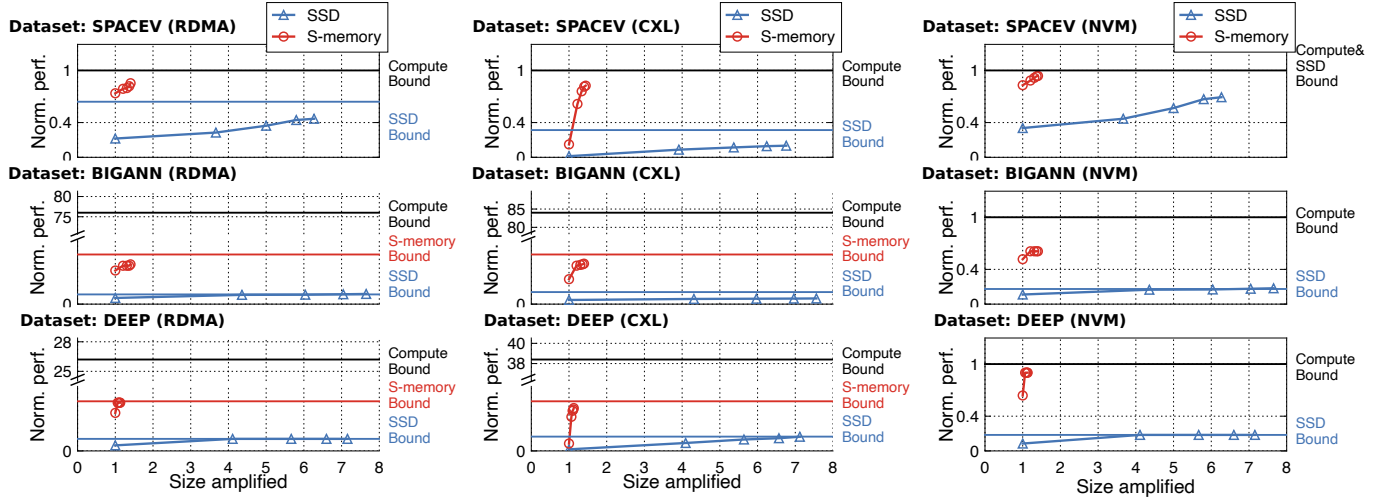


Figure 12: End-to-end cluster index performance. S-memory states for second-tier memory used. We omit the S-memory bound in experiments on the SPACEV dataset and NVM as it is too large (45–430 \times).

6.3 Overall Performance

Effects of grouping. Figure 10 shows the effects of cluster-aware grouping. Specifically, grouping improves the performance on various datasets by 1.3–1.7 \times , and can achieve close or even higher performance than the replicated performance. The improved performance is due to the reduced number of vectors transferred: it reduces 62–80% I/O requests in the chosen workloads.

End-to-end performance. Figure 12 shows the index performance respective to index amplification caused by replicating vectors with all the above optimizations enabled¹⁰. Like graph, we calculate the computation bound by performing all calculations using in-memory data and bandwidth bound by with the peak bandwidth measured in Figure 6. On second-tier memory, cluster index can achieve both high performance and low space utilization with our cluster-aware grouping. Specifically, it only requires 16–22% of the size of the SSD index, and achieves 1.4–7.1 \times higher throughput. Unlike graph index, the bottleneck of the three datasets is quite different on cluster index. SPACEV is bottlenecked by computation in all settings, as it requires reading about only 0.1 MB per query, far less than the other two datasets (0.7 MB and 2.2 MB). This is because it is a skewed dataset where vectors are close. Both BIGANN and DEEP are bottlenecked by second-tier memory bandwidth, as cluster index requires reading more vectors for the search than graph index due to its coarse-grained index nature. Interestingly, on NVM, BIGANN and DEEP are still bottlenecked by the computation power of the CPU, because the equipped CPU is weak (see Table 3).

¹⁰Due to limited memory on our platform, we only report the performance of 100M datasets for CXL.

Table 5: The computational intensity and average bytes read per query vary on different datasets for vector indexes.

| Datasets | Computation intensity | | KBytes Read/query | |
|----------|-----------------------|---------|-------------------|---------|
| | Graph | Cluster | Graph | Cluster |
| SPACEV | 22 | 10 | 32 | 139 |
| BIGANN | 29 | 8 | 38 | 745 |
| DEEP | 19 | 3 | 60 | 2,374 |

7 An end-to-end comparison of graph and cluster index on second-tier memory

An interesting question faced by developers that use vector search is what is the right index—graph or cluster—to choose. For SSD-based vector indexes, a common belief is that graph index is better in storage as it won’t need many edges to achieve a high accuracy [49]. Therefore, developers tend to choose graph index for its smaller index size. In comparison, cluster index requires sufficient replications to achieve the same accuracy level, which is also observed in the paper. For cluster index, a common belief is that it is better in performance as its coarse-grained access pattern is suitable for the SSD. As a result, developers tend to choose cluster index for its higher performance [7, 56].

On second-tier memory, the findings are completely different with our improved index design:

1. Graph index typically has a better IO efficiency on second-tier memory.
2. Cluster index has a small index footprint on second-tier memory.

Performance comparison. Figure 13 shows the end-to-end performance comparison of graph and cluster index on SSD, RDMA, CXL, and NVM with respective to the index size. On BIGANN and DEEP datasets, Graph index is 2.1, 2.2,

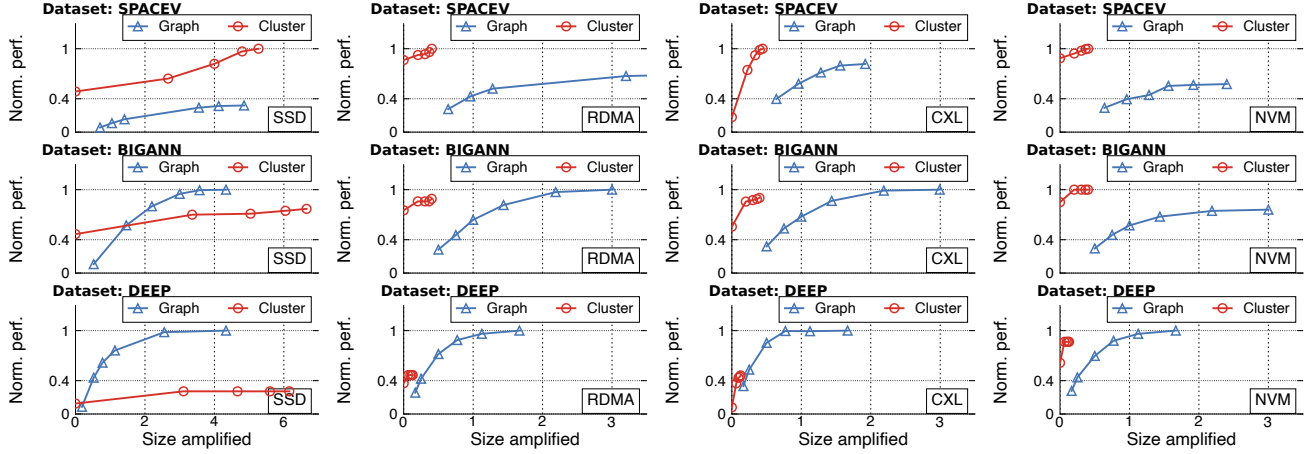


Figure 13: End-to-end comparison of graph and cluster index performance on (a) SSD, (b) RDMA, (c) CXL, and (d) NVM.

and $1.2\times$ faster than cluster on RDMA, CXL, and NVM, respectively. The core reason is that graph reads less data than cluster: on these datasets, graph reads 95–97% fewer bytes than the cluster (see Table 5). Though it decouples such reads into fine-grained I/Os (512–1024 B), they are efficient on second-tier memory, so it is different from the common belief that graph index is slower than cluster. Note that without our software pipeline (§5), graph still cannot outperform cluster due to access delays when traversing the graph.

On SPACEV, cluster index is still 1.5, 1.2, and $1.7\times$ faster than graph on RDMA, CXL, and NVM, respectively. This is because it is a dataset with clusters close in distance. As a result, it only needs to search a few clusters and thus has better performance due to the efficient grouped vector reads enabled by our grouping method.

Space comparison. Thanks to our decoupled layout with group, we nearly eliminated the space amplification caused by the replicated vectors. As a result, on SPACEV, BIGANN, and DEEP datasets, cluster index can achieve optimal performance with only 0.1–0.4 \times index size amplification. This is 56–68% smaller than the graph index. For such amplification, cluster index is a good candidate for index with small amplification on second-tier memory.

8 Related Work

Other vector indexes. A large amount of effort in indexing algorithms has been dedicated to enhancing the efficiency of vector search. Besides the graph and cluster indexes extensively discussed in this paper, tree-based indexing organizes data in a hierarchical tree structure, such as KD-tree[5], Ball-tree[35] or R-tree[20]. Hash-based indexing[55, 21, 17] uses hashing functions to map similar data points to the same buckets, allowing for approximate nearest neighbor queries via hash table lookups. Unfortunately, these indexes cannot either scale to large-scale (e.g., billion-scale) datasets or provide

sufficient accuracy [50, 51].

Vector database. Several systems have been developed to handle the complexities of storing, indexing, and searching high-dimensional vector data. AnalyticDB-V[51], PASE[58] and VBASE[60] integrate vector search into traditional database, allowing for complex queries through SQL syntax. Milvus[48] is an open-source vector database designed to handle embedding vectors converted from unstructured data. Faiss[14] and Annoy[46] developed libraries for efficient vector search. Pinecone[41] is a cloud-native vector database that simplifies the process of building applications with vector search capabilities. SPFresh[56] implements LIRE to support incremental in-place updates for billion-scale vector search. Elasticsearch[13] and Solr[2] can support vector search using algorithms like HNSW in distributed search engines. They are orthogonal to our work, and they use the index built by our study to further enhance the performance of vector search with small index amplifications.

New hardware for vector search. Recently, with the rise of new computation hardware like GPUs and FPGAs, and new I/O hardware like NVM and CXL, many system designers have explored the potential of utilizing them to accelerate vector search [25, 62, 39, 23]. For example, faiss library has proposed a GPU implementation of cluster index to accelerate batched queries. RUMMY is a system that implements efficient compute-IO pipeline to accelerate cluster-based vector search. For graph-based vector search, CAGRA presents a new graph index design that has affinity for parallelism during index construction phase on GPU. They also achieve a performance improvement on CPU-based graph index. CXL-ANNS is a system that utilizes CXL and NDP to accelerate graph-based vector search.

9 Conclusion

Existing large-scale vector indexes on SSD face a dilemma of high performance versus low index amplification, which we attribute to a mismatch between workload requirements and high-performance SSD access patterns. Such a dilemma—though challenging to address from an algorithm’s perspective, can be systematically addressed by a co-design with emerging second-tier memory. Our improved index design can achieve $1.5\text{--}5.6 \times$ performance improvements with 15–62% less index amplification for graph, and $1.4\text{--}5.9 \times$ performance improvements with 92–98% less index amplification for cluster. These results show that second-tier memory is a promising storage medium for vector indexes.

References

[1] ALGORITHMS, A. A. *KGraph: A library for fast approximate nearest neighbor search*, 2014.

[2] APACHE. Solr. <https://solr.apache.org/>, 2024.

[3] ARYA, S., AND MOUNT, D. M. Approximate nearest neighbor queries in fixed dimensions. In *Proceedings of the Fourth Annual ACM/SIGACT-SIAM Symposium on Discrete Algorithms, 25-27 January 1993, Austin, Texas, USA* (1993), V. Ramachandran, Ed., ACM/SIAM, pp. 271–280.

[4] BARROSO, L. A., DEAN, J., AND HÖLZLE, U. Web search for a planet: The google cluster architecture. *IEEE Micro* 23, 2 (2003), 22–28.

[5] BENTLEY, J. L. Multidimensional binary search trees used for associative searching. *Commun. ACM* 18, 9 (1975), 509–517.

[6] CHEN, Q., WANG, H., LI, M., REN, G., LI, S., ZHU, J., LI, J., LIU, C., ZHANG, L., AND WANG, J. *SPTAG: A library for fast approximate nearest neighbor search*, 2018.

[7] CHEN, Q., ZHAO, B., WANG, H., LI, M., LIU, C., LI, Z., YANG, M., AND WANG, J. SPANN: highly-efficient billion-scale approximate nearest neighborhood search. In *Advances in Neural Information Processing Systems 34: Annual Conference on Neural Information Processing Systems 2021, NeurIPS 2021, December 6-14, 2021, virtual* (2021), M. Ranzato, A. Beygelzimer, Y. N. Dauphin, P. Liang, and J. W. Vaughan, Eds., pp. 5199–5212.

[8] CLARKSON, K. L. An algorithm for approximate closest-point queries. In *Proceedings of the Tenth Annual Symposium on Computational Geometry, Stony Brook, New York, USA, June 6-8, 1994* (1994), K. Mehlhorn, Ed., ACM, pp. 160–164.

[9] CLOUD, G. Find anything blazingly fast with google’s vector search technology. <https://cloud.google.com/blog/topics/developers-practitioners/find-anything-blazingly-fast-googles-vector-search-technology>, 2024.

[10] CONSORTIUM, C. Cxl specification. <https://www.computeexpresslink.org/download-the-specification>, 2024.

[11] DEAN, J., AND BARROSO, L. A. The tail at scale. *Commun. ACM* 56, 2 (2013), 74–80.

[12] DRAGOJEVIC, A., NARAYANAN, D., CASTRO, M., AND HODSON, O. Farm: Fast remote memory. In *Proceedings of the 11th USENIX Symposium on Networked Systems Design and Implementation, NSDI 2014, Seattle, WA, USA, April 2-4, 2014* (2014), R. Mahajan and I. Stoica, Eds., USENIX Association, pp. 401–414.

[13] ELASTIC. Elasticsearch. <https://www.elastic.co>, 2024.

[14] FACEBOOK. Faiss. <https://github.com/facebookresearch/faiss>, 2023.

[15] FU, C., XIANG, C., WANG, C., AND CAI, D. Fast approximate nearest neighbor search with the navigating spreading-out graph. *Proc. VLDB Endow.* 12, 5 (jan 2019), 461–474.

[16] GAO, P. X., NARAYAN, A., KARANDIKAR, S., CARREIRA, J., HAN, S., AGARWAL, R., RATNASAMY, S., AND SHENKER, S. Network requirements for resource disaggregation. In *12th USENIX Symposium on Operating Systems Design and Implementation, OSDI 2016, Savannah, GA, USA, November 2-4, 2016* (2016), K. Keeton and T. Roscoe, Eds., USENIX Association, pp. 249–264.

[17] GIONIS, A., INDYK, P., AND MOTWANI, R. Similarity search in high dimensions via hashing. In *VLDB’99, Proceedings of 25th International Conference on Very Large Data Bases, September 7-10, 1999, Edinburgh, Scotland, UK* (1999), M. P. Atkinson, M. E. Orlowska, P. Valduriez, S. B. Zdonik, and M. L. Brodie, Eds., Morgan Kaufmann, pp. 518–529.

[18] GOUK, D., LEE, S., KWON, M., AND JUNG, M. Direct access, high-performance memory disaggregation with directcxl. In *2022 USENIX Annual Technical Conference, USENIX ATC 2022, Carlsbad, CA, USA, July 11-13, 2022* (2022), J. Schindler and N. Zilberman, Eds., USENIX Association, pp. 287–294.

[19] GU, J., LEE, Y., ZHANG, Y., CHOWDHURY, M., AND SHIN, K. G. Efficient memory disaggregation with infiniswap. In *14th USENIX Symposium on Networked Systems Design and Implementation, NSDI 2017, Boston, MA, USA, March 27-29, 2017* (2017), A. Akella and J. Howell, Eds., USENIX Association, pp. 649–667.

[20] GUTTMAN, A. R-trees: A dynamic index structure for spatial searching. In *SIGMOD’84, Proceedings of Annual Meeting, Boston, Massachusetts, USA, June 18-21, 1984* (1984), B. Yormark, Ed., ACM Press, pp. 47–57.

[21] HUANG, Q., FENG, J., ZHANG, Y., FANG, Q., AND NG, W. Query-aware locality-sensitive hashing for approximate nearest neighbor search. *Proc. VLDB Endow.* 9, 1 (2015), 1–12.

[22] IZRAELEVITZ, J., YANG, J., ZHANG, L., KIM, J., LIU, X., MEMARIPOUR, A. S., SOH, Y. J., WANG, Z., XU, Y., DULLOOR, S. R., ZHAO, J., AND SWANSON, S. Basic performance measurements of the intel optane DC persistent memory module. *CoRR abs/1903.05714* (2019).

[23] JANG, J., CHOI, H., BAE, H., LEE, S., KWON, M., AND JUNG, M. CXL-ANNS: software-hardware collaborative memory disaggregation and computation for billion-scale approximate nearest neighbor search. In *2023 USENIX Annual Technical Conference, USENIX ATC 2023, Boston, MA, USA, July 10-12, 2023* (2023), J. Lawall and D. Williams, Eds., USENIX Association, pp. 585–600.

[24] JOHN FORREST, R. L.-H. Cbc user guide. <https://www.coin-or.org/Cbc/cbcuserguide.html>, 2024.

[25] JOHNSON, J., DOUZE, M., AND JÉGOU, H. Billion-scale similarity search with gpus. *IEEE Trans. Big Data* 7, 3 (2021), 535–547.

[26] JUN, Y., PARK, S., KANG, J., KIM, S., AND SEO, E. We ain't afraid of no file fragmentation: Causes and prevention of its performance impact on modern flash ssds. In *22nd USENIX Conference on File and Storage Technologies, FAST 2024, Santa Clara, CA, USA, February 27-29, 2024* (2024), X. Ma and Y. Won, Eds., USENIX Association, pp. 193–208.

[27] KALIA, A., KAMINSKY, M., AND ANDERSEN, D. G. Design guidelines for high performance RDMA systems. *login Usenix Mag.* 41, 3 (2016).

[28] KALIA, A., KAMINSKY, M., AND ANDERSEN, D. G. Fasst: Fast, scalable and simple distributed transactions with two-sided (RDMA) datagram rpcs. In *12th USENIX Symposium on Operating Systems Design and Implementation, OSDI 2016, Savannah, GA, USA, November 2-4, 2016* (2016), K. Keeton and T. Roscoe, Eds., USENIX Association, pp. 185–201.

[29] LANDRUM, B. Ivf2 index: Fusing classic and spatial inverted indices for fast filtered anns. https://big-ann-benchmarks.com/neurips23_slides/IVF_2_filter_Ben.pdf, 2024.

[30] LEWIS, P. S. H., PEREZ, E., PIKTUS, A., PETRONI, F., KARPUKHIN, V., GOYAL, N., KÜTTLER, H., LEWIS, M., YIH, W., ROCKTÄSCHEL, T., RIEDEL, S., AND KIELA, D. Retrieval-augmented generation for knowledge-intensive NLP tasks. In *Advances in Neural Information Processing Systems 33: Annual Conference on Neural Information Processing Systems 2020, NeurIPS 2020, December 6-12, 2020, virtual* (2020), H. Larochelle, M. Ranzato, R. Hadsell, M. Balcan, and H. Lin, Eds.

[31] LI, H., BERGER, D. S., HSU, L., ERNST, D., ZARDOSHTI, P., NOVAKOVIC, S., SHAH, M., RAJADNYA, S., LEE, S., AGARWAL, I., HILL, M. D., FONTOURA, M., AND BIANCHINI, R. Pond: Cxl-based memory pooling systems for cloud platforms. In *Proceedings of the 28th ACM International Conference on Architectural Support for Programming Languages and Operating Systems, Volume 2, ASPLOS 2023, Vancouver, BC, Canada, March 25-29, 2023* (2023), T. M. Aamodt, N. D. E. Jerger, and M. M. Swift, Eds., ACM, pp. 574–587.

[32] LI, S., LV, F., JIN, T., LIN, G., YANG, K., ZENG, X., WU, X., AND MA, Q. Embedding-based product retrieval in taobao search. In *KDD '21: The 27th ACM SIGKDD Conference on Knowledge Discovery and Data Mining, Virtual Event, Singapore, August 14-18, 2021* (2021), F. Zhu, B. C. Ooi, and C. Miao, Eds., ACM, pp. 3181–3189.

[33] LI, W., ZHANG, Y., SUN, Y., WANG, W., LI, M., ZHANG, W., AND LIN, X. Approximate nearest neighbor search on high dimensional data — experiments, analyses, and improvement. *IEEE Transactions on Knowledge and Data Engineering* 32, 8 (2020), 1475–1488.

[34] LIU, H., HUANG, Z., CHEN, Q., LI, M., FU, Y., AND ZHANG, L. Fast clustering with flexible balance constraints. In *IEEE International Conference on Big Data (IEEE Big-Data 2018), Seattle, WA, USA, December 10-13, 2018* (2018), N. Abe, H. Liu, C. Pu, X. Hu, N. K. Ahmed, M. Qiao, Y. Song, D. Kossmann, B. Liu, K. Lee, J. Tang, J. He, and J. S. Saltz, Eds., IEEE, pp. 743–750.

[35] LIU, T., MOORE, A. W., AND GRAY, A. G. New algorithms for efficient high-dimensional nonparametric classification. *J. Mach. Learn. Res.* 7 (2006), 1135–1158.

[36] MALKOV, Y. A., AND YASHUNIN, D. A. Efficient and robust approximate nearest neighbor search using hierarchical navigable small world graphs. *IEEE transactions on pattern analysis and machine intelligence* 42, 4 (2018), 824–836.

[37] MARUF, H. A., WANG, H., DHANOTIA, A., WEINER, J., AGARWAL, N., BHATTACHARYA, P., PETERSEN, C., CHOWDHURY, M., KANAUJIA, S. O., AND CHAUHAN, P. TPP: transparent page placement for cxl-enabled tiered-memory. In *Proceedings of the 28th ACM International Conference on Architectural Support for Programming Languages and Operating Systems, Volume 3, ASPLOS 2023, Vancouver, BC, Canada, March 25-29, 2023* (2023), T. M. Aamodt, N. D. E. Jerger, and M. M. Swift, Eds., ACM, pp. 742–755.

[38] MIKOLOV, T., CHEN, K., CORRADO, G., AND DEAN, J. Efficient estimation of word representations in vector space. In *1st International Conference on Learning Representations, ICLR 2013, Scottsdale, Arizona, USA, May 2-4, 2013, Workshop Track Proceedings* (2013), Y. Bengio and Y. LeCun, Eds.

[39] OOTOMO, H., NARUSE, A., NOLET, C., WANG, R., FEHER, T., AND WANG, Y. CAGRA: highly parallel graph construction and approximate nearest neighbor search for gpus. *CoRR abs/2308.15136* (2023).

[40] PENNINGTON, J., SOCHER, R., AND MANNING, C. D. Glove: Global vectors for word representation. In *Proceedings of the 2014 Conference on Empirical Methods in Natural Language Processing, EMNLP 2014, October 25-29, 2014, Doha, Qatar, A meeting of SIGDAT, a Special Interest Group of the ACL* (2014), A. Moschitti, B. Pang, and W. Daelemans, Eds., ACL, pp. 1532–1543.

[41] PINECONE. Pinecone. <https://www.pinecone.io>, 2024.

[42] REN, J., ZHANG, M., AND LI, D. HM-ANN: efficient billion-point nearest neighbor search on heterogeneous memory. In *Advances in Neural Information Processing Systems 33: Annual Conference on Neural Information Processing Systems 2020, NeurIPS 2020, December 6-12, 2020, virtual* (2020), H. Larochelle, M. Ranzato, R. Hadsell, M. Balcan, and H. Lin, Eds.

[43] SAAD, Y. *Iterative methods for sparse linear systems*. SIAM, 2003.

[44] SHEWALE, R. Google search statistics 2024 (no. of searches per day). <https://www.demandsage.com/google-search-statistics/>, 2024.

[45] SPDK. Build ultra high-performance storage applications with the storage performance development kit. <https://spdk.io>, 2024.

[46] SPOTIFY. Annoy. <https://github.com/spotify/annoy>, 2024.

[47] SUBRAMANYA, S. J., DEVVRIT, KADEKODI, R., KRISHASWAMY, R., AND SIMHADRI, H. V. *DiskANN: Fast Accurate Billion-Point Nearest Neighbor Search on a Single Node*. Curran Associates Inc., Red Hook, NY, USA, 2019.

[48] WANG, J., YI, X., GUO, R., JIN, H., XU, P., LI, S., WANG, X., GUO, X., LI, C., XU, X., YU, K., YUAN, Y., ZOU, Y., LONG, J., CAI, Y., LI, Z., ZHANG, Z., MO, Y., GU, J., JIANG, R., WEI, Y., AND XIE, C. Milvus: A purpose-built vector data management system. In *Proceedings of the 2021 International Conference on Management of Data* (New York, NY, USA, 2021), SIGMOD '21, Association for Computing Machinery, p. 2614–2627.

[49] WANG, M., XU, W., YI, X., WU, S., PENG, Z., KE, X., GAO, Y., XU, X., GUO, R., AND XIE, C. Starling: An i/o-efficient disk-resident graph index framework for high-dimensional vector similarity search on data segment. *CoRR abs/2401.02116* (2024).

[50] WEBER, R., SCHEK, H., AND BLOTT, S. A quantitative analysis and performance study for similarity-search methods in high-dimensional spaces. In *VLDB'98, Proceedings of 24rd International Conference on Very Large Data Bases, August 24-27, 1998, New York City, New York, USA* (1998), A. Gupta, O. Shmueli, and J. Widom, Eds., Morgan Kaufmann, pp. 194–205.

[51] WEI, C., WU, B., WANG, S., LOU, R., ZHAN, C., LI, F., AND CAI, Y. Analyticdb-v: A hybrid analytical engine towards query fusion for structured and unstructured data. *Proc. VLDB Endow.* 13, 12 (aug 2020), 3152–3165.

[52] WEI, X., DONG, Z., CHEN, R., AND CHEN, H. Deconstructing RDMA-enabled distributed transactions: Hybrid is better! In *13th USENIX Symposium on Operating Systems Design and Implementation (OSDI 18)* (Carlsbad, CA, Oct. 2018), USENIX Association, pp. 233–251.

[53] WEI, X., XIE, X., CHEN, R., CHEN, H., AND ZANG, B. Characterizing and optimizing remote persistent memory with RDMA and NVM. In *2021 USENIX Annual Technical Conference, USENIX ATC 2021, July 14-16, 2021* (2021), I. Calciu and G. Kuenning, Eds., USENIX Association, pp. 523–536.

[54] WEI, X., XIE, X., CHEN, R., CHEN, H., AND ZANG, B. Characterizing and optimizing remote persistent memory with RDMA and NVM. In *2021 USENIX Annual Technical Conference, USENIX ATC 2021, July 14-16, 2021* (2021), I. Calciu and G. Kuenning, Eds., USENIX Association, pp. 523–536.

[55] WEISS, Y., TORRALBA, A., AND FERGUS, R. Spectral hashing. In *Advances in Neural Information Processing Systems 21, Proceedings of the Twenty-Second Annual Conference on Neural Information Processing Systems, Vancouver, British Columbia, Canada, December 8-11, 2008* (2008), D. Koller, D. Schuurmans, Y. Bengio, and L. Bottou, Eds., Curran Associates, Inc., pp. 1753–1760.

[56] XU, Y., LIANG, H., LI, J., XU, S., CHEN, Q., ZHANG, Q., LI, C., YANG, Z., YANG, F., YANG, Y., CHENG, P., AND YANG, M. Spfresh: Incremental in-place update for billion-scale vector search. In *Proceedings of the 29th Symposium on Operating Systems Principles, SOSP 2023, Koblenz, Germany, October 23-26, 2023* (2023), J. Flinn, M. I. Seltzer, P. Druschel, A. Kaufmann, and J. Mace, Eds., ACM, pp. 545–561.

[57] YANG, J., KIM, J., HOSEINZADEH, M., IZRAELEVITZ, J., AND SWANSON, S. An empirical guide to the behavior and use of scalable persistent memory. In *18th USENIX Conference on File and Storage Technologies, FAST 2020, Santa Clara, CA, USA, February 24-27, 2020* (2020), S. H. Noh and B. Welch, Eds., USENIX Association, pp. 169–182.

[58] YANG, W., LI, T., FANG, G., AND WEI, H. PASE: postgresql ultra-high-dimensional approximate nearest neighbor search extension. In *Proceedings of the 2020 International Conference on Management of Data, SIGMOD Conference 2020, online conference [Portland, OR, USA], June 14-19, 2020* (2020), D. Maier, R. Pottinger, A. Doan, W. Tan, A. Alawini, and H. Q. Ngo, Eds., ACM, pp. 2241–2253.

[59] ZHANG, H., ANDERSEN, D. G., PAVLO, A., KAMINSKY, M., MA, L., AND SHEN, R. Reducing the storage overhead of main-memory OLTP databases with hybrid indexes. In *Proceedings of the 2016 International Conference on Management of Data, SIGMOD Conference 2016, San Francisco, CA, USA, June 26 - July 01, 2016* (2016), F. Özcan, G. Koutrika, and S. Madden, Eds., ACM, pp. 1567–1581.

[60] ZHANG, Q., XU, S., CHEN, Q., SUI, G., XIE, J., CAI, Z., CHEN, Y., HE, Y., YANG, Y., YANG, F., YANG, M., AND ZHOU, L. VBASE: Unifying online vector similarity search and relational queries via relaxed monotonicity. In *17th USENIX Symposium on Operating Systems Design and Implementation (OSDI 23)* (Boston, MA, July 2023), USENIX Association, pp. 377–395.

[61] ZHANG, Y., RUAN, C., LI, C., YANG, J., CAO, W., LI, F., WANG, B., FANG, J., WANG, Y., HUO, J., AND BI, C. Towards cost-effective and elastic cloud database deployment via memory disaggregation. *Proc. VLDB Endow.* 14, 10 (2021), 1900–1912.

[62] ZHANG, Z., LIU, F., HUANG, G., LIU, X., AND JIN, X. Fast vector query processing for large datasets beyond GPU memory with reordered pipelining. In *21st USENIX Symposium on Networked Systems Design and Implementation, NSDI 2024, Santa Clara, CA, April 15-17, 2024* (2024), L. Vanbever and I. Zhang, Eds., USENIX Association, pp. 23–40.

[63] ZUO, P., SUN, J., YANG, L., ZHANG, S., AND HUA, Y. One-sided rdma-conscious extendible hashing for disaggregated memory. In *2021 USENIX Annual Technical Conference (USENIX ATC 21)* (July 2021), USENIX Association, pp. 15–29.